ACS Sustainable Chemistry & Engineering

pubs.acs.org/journal/ascecg

Research Article

Solvometallurgical Recovery of Platinum Group Metals from Spent Automotive Catalysts

Viet Tu Nguyen, Sofía Riaño, Emir Aktan, Clio Deferm, Jan Fransaer, and Koen Binnemans*

Cite This: *ACS Sustainable Chem. Eng.* 2021, 9, 337−350

Read Online

ACCESS | Metrics & More | Article Recommendations | Supporting Information

ABSTRACT: Extraction and separation of platinum group metals (PGMs) from secondary raw materials are usually carried out via hydrometallurgical processes. These processes use strongly oxidizing acidic solutions, such as *aqua regia* or hydrochloric acid in the presence of chlorine gas, which may have negative environmental impacts and are dangerous. In this paper, a solvometallurgical approach was developed for the sustainable recovery of PGMs from spent automotive exhaust catalysts. The PGMs were leached using $FeCl_3$ or $CuCl_2$ as oxidizing agents in the organic solvents dimethyl sulfoxide (DMSO) or acetonitrile (CH_3CN). Palladium was quantitatively dissolved in $CuCl_2/CH_3CN$, $CuCl_2$/DMSO, and $FeCl_3$/DMSO with only 10−20% codissolution of Pt and Rh. By adjusting the concentration of the oxidizing agent in CH_3CN, Pd was selectively leached with 0.01 mol L^{-1} $FeCl_3$, whereas Pt and Rh could be dissolved in a more concentrated $FeCl_3$ solution (0.3 mol L^{-1}). The solvoleaching of PGMs was investigated in depth by UV−vis spectra and electrochemical properties (*i.e.*, cyclic voltammograms and formal reduction potentials of the Fe^{3+}/Fe^{2+} and Cu^{2+}/Cu^{+} couples in DMSO and CH_3CN). After leaching, CH_3CN was easily recovered by distillation. The Pd-containing residue was dissolved in water, from which Pd sponge was produced by reduction with formic acid. Meanwhile, the residue containing the solid chloride salts of Fe(III), Pt(IV), and Rh(III) was redissolved in ethylene glycol or DMSO for further purification by nonaqueous solvent extraction (NASX). The ionic liquid Aliquat 336 diluted in *p*-cymene showed selective extraction of Fe(III) and Pt(IV) while leaving Rh(III) in the raffinate. The loaded ionic liquid was recycled after selective stripping of Fe(III) with water and Pt(IV) with a thiourea solution. A flow sheet comprising solvoleaching and NASX is proposed. The closed-loop solvoleaching of PGMs with less-hazardous chemicals ($FeCl_3/CH_3CN$) avoids the emission of toxic or flammable gases (Cl_2, H_2, and NO_x) while reducing the consumption of acids and bases and limiting the generation of waste water. In addition, NASX with an ionic liquid may be a more sustainable alternative for the conventional separation of PGMs.

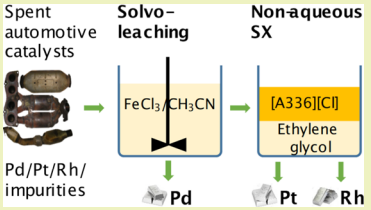

KEYWORDS: *nonaqueous solvent extraction, oxidative leaching, precious metals, recycling, solvometallurgy*

INTRODUCTION

The platinum group metals (PGMs) platinum, palladium, and rhodium are primarily used in clean technologies and high-tech equipment. An important application of these PGMs is automotive catalytic converters, which substantially reduce the exhaust pollutant emissions of CO, NO_x, and hydrocarbons from the internal combustion engines by converting these compounds into CO_2, N_2, and H_2O, respectively.[1] Currently, the demand of PGMs for industrial applications has increased on account of stricter environmental legislations. Because of their supply risk and their economic importance, PGMs have been classified as critical elements by the European Commission.[2] Effective recycling systems for PGM-containing secondary raw materials are of great importance to ensure the sustainable supply of the precious metals.

Extensive efforts have been made to develop energy-efficient and eco-friendly pyro- and/or hydrometallurgical processes to recover PGMs from spent automotive catalysts converters.[3−6] In industry, PGMs are usually recovered in smelting furnaces with base metals (*i.e.*, Cu, Ni, and Pb) as collectors.[7] The PGM-enriched alloy is then refined by hydrometallurgical methods to recover the individual metals. Because pyrometallurgical processes are energy-intensive and generate large quantities of slag and environmental pollutants (*i.e.*, SO_2, NO_x, CO, and dioxins),[3] full hydrometallurgical flow sheets are being developed for recovery of PGMs from spent car exhaust catalysts.[8]

Because of their chemical refractory, the direct dissolution of PGMs in a refinery requires strongly oxidizing conditions: (i) *aqua regia* (HCl/HNO_3 in 3:1 molar ratio) or (ii) concentrated acids (HCl and H_2SO_4) in the presence of oxidizing agents (*i.e.*, Cl_2, H_2O_2, $HClO_4$, NaClO, $NaClO_3$, and $NaBrO_3$).[9−12] The dissolution of PGMs in *aqua regia* raises environmental concerns because of the formation of highly toxic chlorine and nitrous gases (*i.e.*, Cl_2, NOCl, HNO_2, NO, and NO_2).[13] Recently, the oxidative leaching of Pd and Rh from spent catalytic converters was achieved using Cu(II) in

Received: October 7, 2020
Revised: December 7, 2020
Published: December 28, 2020

hydrochloric acid.[14] Up to 95% Pd and 86% Rh were dissolved in Cu(II)/HCl under optimized conditions (6 mol L^{-1} HCl, 0.3 mol L^{-1} Cu(II), 80 °C, and 4 h). A disadvantage of this process is the use of concentrated HCl, which can be harmful for the environment and is corrosive toward equipment.

Solvometallurgy is an emerging branch of extractive metallurgy, which focuses on the recovery of metals using nonaqueous solutions.[15] Because of the absence of a discrete water phase, the solvating properties of a system change significantly. This implies that the mechanisms of extraction in solvometallurgical processes differ from those in hydrometallurgical ones. The difference in the metal extraction mechanism can be exploited for the selective leaching of metals.[15] For instance, oxidative leaching was used for the selective dissolution of metals (*i.e.*, uranium, rhenium, zirconium, and copper) in organic solvents (*i.e.*, bromide−ethyl acetate, bromide−methanol, chlorine−$FeCl_3$−dimethylformamide, and $FeCl_3$−ethylene glycol).[16−19] Recent work of our research group showed that different metals can be dissolved in trihalide ionic liquids, with the trichloride compounds as the most reactive ones.[20,21] Nakao et al. studied the dissolution of noble metals using elemental halogens and halides dissolved in polar organic solvents.[22] The quantitative recovery of palladium from spent catalytic converters can also be achieved using *N*,*N*′-dimethylperhydrodiazepine-2,3-dithione diiodine.[23] However, because of their high reactivity, halogens can attack the organic solvents and form hazardous halogenated byproducts. Mixtures of $SOCl_2$ with pyridine, *N*,*N*-dimethylformamide (DMF), pyrimidine, or imidazole have been used to dissolve gold, silver, and palladium. Interestingly, "*organic aqua regia*" allows the selective separation of platinum from palladium.[24]

After the oxidative dissolution of PGMs, the mixture of PGMs must be separated into individual elements. In conventional solvent extraction, the aqueous pregnant leach solution is contacted with an immiscible organic phase that is mainly composed of an extractant [*i.e.*, MIBK, a mixture of quaternary ammonium chlorides (Aliquat 336 or [A336][Cl]), trioctylamine (TOA), tri-*n*-butylphosphate (TBP), Cyanex 921, Cyanex 923, LIX 84I, and dialkyl sulphoxides] and a diluent. The separation of the individual PGMs, however, has several bottlenecks: (i) slow kinetics, (ii) poor selectivity, (iii) high chemical consumption, and (iv) high waste generation.[25] Therefore, *nonaqueous solvent extraction* (NASX) has been proposed as an alternative to the conventional processes.[15] In NASX, two immiscible organic phases are contacted. The more polar phase [*i.e.*, dimethyl sulfoxide (DMSO), acetonitrile (CH_3CN), ethylene glycol (EG), polyethylene glycol (PEG), methanol (CH_3OH), and dimethylformamide (DMF)] contains the metals to be extracted. Meanwhile, the less-polar phase consists of an extractant [*i.e.*, TBP, Cyanex 923, TOA, LIX 984, [A336][Cl], and trihexyl(tetradecyl)phosphonium chloride (Cyphos IL 101 or [P66614][Cl])] and a diluent (*i.e.*, *p*-cymene, GS 190, dodecane, or kerosene). Careful choice of the solvents for NASX is crucial to assure the sustainability of the process. The preferred solvent pairs must have (i) low environmental impact, (ii) low mutual solubility, (iii) rapid phase disengagement, (iv) good solubility of the extractant in the less-polar phase, and (v) good solubility of the to-be-extracted metal salts in the more-polar phase.[15] Recent studies on NASX have shown that selectivity can be quite different from that observed in conventional extraction from aqueous feed solutions.[26−29]

In this paper, an integrated solvometallurgical process comprising solvoleaching and NASX is developed for the sustainable recovery of PGMs from spent automotive catalysts. The selective dissolution of PGMs is studied using different solvents (DMSO and CH_3CN) in the presence of oxidizing reagents ($FeCl_3$ and $CuCl_2$) under different conditions (*i.e.*, temperature, leaching time, oxidizing agent concentration, and solid-to-liquid ratio). DMSO and CH_3CN are chosen because they have a relative low toxicity and can easily be regenerated and produced in large quantities. In addition, safe and cheap oxidizing agents (*i.e.*, $FeCl_3$ and $CuCl_2$) that avoid the emission of toxic gases (*i.e.*, Cl_2, H_2, and NO_x) during the dissolution also contribute to the greenness of the process. After leaching, the PGMs are separated into individual elements using NASX. A conceptual flow sheet is presented for recycling PGMs from spent automotive catalysts.

EXPERIMENTAL SECTION

Materials. A representative sample of spent automotive catalysts (particle size < 0.16 mm) was kindly provided by Monolithos Catalysts Ltd. (Greece). The preparation procedure of this sample was reported by Yakoumis et al.[30] Dimethylsulfoxide (DMSO, ≥99.7%), copper(II) chloride (anhydrous, ≥98%), iron(III) chloride (anhydrous, ≥98%), iron(II) chloride (anhydrous, 97%), thiourea (≥99%), *p*-cymene (≥99%), and 1,10-phenanthroline were obtained from ACROS Organics (Geel, Belgium). Acetonitrile (CH_3CN, ≥99.5%) and ammonia solution (25 wt %) were purchased from Chem-Lab NV (Zedelgem, Belgium). Hydrochloric acid (HCl, 37 wt %) and nitric acid (HNO_3, 68 wt %) were ordered from VWR Chemicals (Leuven, Belgium). Cyanex 923 (a commercial mixture of trialkylphosphine oxides with C_6 and C_8 chains) was provided by Cytec Industries (Canada). TBP was obtained from Alfa Aesar (USA). Aliquat 336 ([A336][Cl], a commercial mixture of quaternary ammonium chlorides with 88.2−90.6%) and TOA (≥98%) were obtained from Sigma-Aldrich (Diegem, Belgium). Trihexyl(tetradecyl)phosphonium chloride (Cyphos IL 101, >97%) was purchased from Cytec Industries Inc. (Niagara Falls, Ontario, Canada). LIX 984 reagent (a mixture 1:1 v/v of 5-nonylsalicylaldoxime and 2-hydroxy-5-nonyl-acetophenone oxime) was obtained from BASF (Germany). Standard solutions of individual metals for inductively coupled plasma optical emission spectrometry (ICP−OES) analysis (*i.e.*, 1000 mg L^{-1} Pt, Pd, Rh, Al, Mg, Ce, Zr, Ca, Fe, Zn, Ni, Cu, Cr, As, Mn, Pb, Sc, and Co in 2% wt % HNO_3), ethylene glycol (EG, anhydrous, ≥99.8%), polyethylene glycol, average molecular weight 200 (PEG-200, ≥99%), tetrafluoroboric acid solution (HBF_4, 48 wt % in H_2O), tetraethylammonium bis(trifluoromethylsulfonyl)imide (>99.0%), tetrabutylammonium perchlorate (>99.0%), and hydrogen peroxide solution (H_2O_2, 30 wt % in H_2O) were purchased from Sigma-Aldrich (Diegem, Belgium). Silver nitrate ($AgNO_3$, >99.5%) was ordered from Honeywell Fluka (Leuven, Belgium). All chemicals and reagents were of analytical grade and used as received, without any further purification.

Characterization of Spent Automotive Catalysts. The mineralogy of the spent automotive catalysts was measured using an X-ray powder diffractometer (Bruker, D2 PHASER) with a Cu Kα X-ray tube operated at 30 kV and 10 mA (Figure S1). The distribution and composition of the PGMs and other elements in the catalyst samples were semiquantitatively analyzed with a field emission electron probe microanalyzer (Jeol JXA-8530F), which uses a high-energy focused beam of electrons to generate X-rays at 15 kV acceleration voltage and 50 nA probe current. The EPMA element mapping and the point analysis of the starting material are shown in Figures S2 and S3, respectively. The quantitative chemical characterization of the spent automotive catalyst powder was performed in triplicate using a Speedwave XPERT microwave digester (Berghof, Germany). A total of 100 mg of the sample was weighted and put in a DAK-100X pressure vessel. Subsequently, 5 mL of hydrochloric acid (HCl, 37 wt %), 4.5 mL of nitric acid (HNO_3, 68 wt %), 3 mL of

https://dx.doi.org/10.1021/acssuschemeng.0c07355
ACS Sustainable Chem. Eng. 2021, 9, 337−350

tetrafluoroboric acid (HBF_4, 48 wt %), and 3 mL of hydrogen peroxide (H_2O_2, 30 % wt %) were slowly added to the vessel. Complete dissolution of the sample was achieved with the digestion program presented in Table S2. After digestion, the solution was cooled down and diluted with concentrated HCl in a 25 mL volumetric flask. Metal concentrations were determined by ICP−OES using a PerkinElmer Optima 8300 spectrometer equipped with a GemTip Cross-Flow II nebulizer, Scott doublepass spray chamber, alumina injector, and PerkinElmer Hybrid XLT ceramic-quartz torch. Both the radial and axial viewing modes were used for all measurements. The lines at 214.423, 363.470, and 343.489 nm were used for the determination of Pt, Pd, and Rh, respectively. The calibration curve was constructed using four calibration standards at 0.01, 0.1, 1.0, and 10 mg L^{-1} and by fitting through the origin. Yttrium (5.0 mg L^{-1}) was used as an internal standard in 2% v/v HNO_3. Quality control samples were run after calibration and every 10 measurements to verify the performance of the instrument. All ICP samples were measured in triplicate.

Solvoleaching of Spent Automotive Catalysts. A total of 100 mg of the sample of spent automotive catalysts was placed in a 4.5 mL vial and 1.0 mL of lixiviant (*i.e.*, 0.01−0.3 mol L^{-1} $FeCl_3$ or 0.01−0.08 mol L^{-1} $CuCl_2$ in CH_3CN, DMSO, EG, and PEG) was added. The vial was closed and the mixture was stirred during 3 h at 700 rpm and 70 °C using a stirring heating plate. After leaching, the leachate and the solid residue were separated with a Heraeus Labofuge 200 centrifuge (Thermo Fisher Scientific, Asse, Belgium) followed by filtration with a 0.45 μm syringe filter (CHROMAFIL Xtra PET-45/25). The filtrate containing the PGMs was diluted using 2% v/v HNO_3 and characterized with ICP−OES. In the case of CH_3CN, the solvent was first evaporated using a rotary evaporator, and afterward, the residue was reconstituted using 2% v/v HNO_3 and analyzed by ICP−OES. The Fourier transform infrared (FTIR) spectra of the metal complexes in organic solvents were recorded on a Bruker Vertex 70 spectrometer in the wavenumber range from 4000 to 400 cm^{-1}. The concentration of Fe(II) in the leachates was quantified using an Agilent Cary 6000i UV−vis−NIR spectrometer with 1,10-phenanthroline as a colorimetric agent.[19] The samples were prepared by mixing a certain volume of the leachate with 1 mL of 1,10-phenanthroline solution (0.5 wt % in CH_3CN) and 1 mL of buffer solution (1: 1 v/v of 5 mol L^{-1} NaOH and 6 mol L^{-1} CH_3COOH, pH = 3.5). The mixture was then diluted with milliQ water to 10 mL. The standard solutions of Fe(II) in the range 1−5 mg L^{-1} were prepared from $FeCl_2$ diluted in the same matrix. The *leaching efficiency* (% *L*) of each metal was calculated based on the mass ratio, as shown in eq 1

$$\%\, L = \frac{m_{aq}}{m_0} \times 100 \tag{1}$$

where m_0 is the total mass of the metal in the starting material and m_{aq} is the mass of the metal in the leachate.

Electrochemical Study. All the electrochemical experiments were carried out using a three-electrode setup at room temperature. For voltammetry experiments, the counter electrode used was a glassy carbon (GC) plate/rod. The working electrode used was a GC rod imbedded in glass with a free surface area of 0.785 mm^2 or a platinum plate with a surface area ranging from 22 to 48 mm^2. The cathodic (E_{red}) and anodic (E_{ox}) limiting potentials were determined by a graphical method at the potential value where tangent lines to the main reduction/oxidation peaks and the horizontal baseline at the "flat" electroactivity domains cross. Redox reaction potentials were determined by the same method. The limiting potentials of the electrochemical window were represented in the figures by vertical dashed lines. Unless stated otherwise, all cyclic voltammograms (CVs) were measured starting at open-circuit potential (OCP) and by scanning first in the cathodic direction.

The polarization curves were recorded in the potential range from −600 to +600 mV with respect to the OCP for the 0.08 mol L^{-1} $FeCl_3/CH_3CN$ system and in the potential range −600 to +1000 mV with respect to the OCP for the 0.08 mol L^{-1} $CuCl_2/CH_3CN$ system at a scan rate of 1 mV/s. The corrosion potential (E_{corr}) and corrosion current (i_{corr}) were obtained from Tafel analyses based on the polarization curves.

For all electrochemical experiments, a silver wire immersed in an solution of 0.01 M $AgNO_3$ and 0.1 M Bu_4NClO_4 in DMSO or CH_3CN was used as a reference electrode. The DMSO or CH_3CN solution containing the Ag/Ag^+ redox couple was placed inside a glass tube with a glass frit on the bottom. Before the experiments, the GC and Pt substrates were rinsed for 5 min with hydrochloric acid (6 mol L^{-1}), deionized water, and ethanol and finally dried in a stream of hot air. The electrochemical experiments were performed using a Metrohm Autolab PGSTAT 302N potentiostat controlled with NOVA 1.11 software.

Nonaqueous Solvent Extraction. The leachate that was obtained after dissolution of the spent automotive catalysts with $FeCl_3$ in CH_3CN was first evaporated to dryness using a rotary evaporator to recover the CH_3CN. Afterward, the solid was redissolved in different polar phases such as DMSO or EG. Subsequently, several parameters of NASX were investigated for the separation of PGMs using common extractants (*i.e.*, [A336][Cl], [P66614][Cl], TBP, Cyanex 923, TOA, and LIX 984) diluted in *p*-cymene. A total of 1.0 mL of the less-polar phase and 1.0 mL of the more polar phase were mixed in a 4.5 mL vial at 25 °C and 2000 rpm for 60 min to ensure equilibrium, unless stated otherwise. The phase disengagement after extraction was accelerated using a Heraeus Labofuge 200 centrifuge at 5000 rpm for 5 min. The raffinate was then separated and diluted in 2% v/v HNO_3 to determine metal content with ICP−OES. The *percentage extraction* (%*E*) is expressed as

$$\%\, E = \frac{[M]_{ini,polar} - [M]_{eq,polar}}{[M]_{eq,polar}} \times 100 \tag{2}$$

where $[M]_{ini,polar}$ and $[M]_{eq,polar}$ are the initial and equilibrium concentration of metals in the more polar phases, respectively.

The stripping experiments were performed by equilibrating individual stripping solutions such as water, thiourea/HCl, HCl, NH_3 (aq), and $Na_2S_2O_3$ with the loaded less-polar organic phases at certain phase ratios in 4.5 mL vials at 25 °C and 2000 rpm for 60 min to ensure equilibrium. After phase separation, the aqueous phase was separated and diluted in 2% v/v HNO_3 for further analysis by ICP−OES. The *percentage stripping* (% *S*) is defined as

$$\%\, S = \frac{[M]_{st,aq} V_{aq}}{[M]_{0,org} V_{org}} \times 100 \tag{3}$$

where $[M]_{0,org}$ represents the total concentration of metal in the loaded organic phase before stripping and $[M]_{st,aq}$ is the concentration of metal in the strip product solution and V_{org} and V_{aq} are the volume of the organic phase and the aqueous phase, respectively.

RESULTS AND DISCUSSION

Characterization of the Spent Automotive Catalysts. The X-ray diffraction (XRD) pattern showed the presence of cordierite $Mg_2Al_4Si_5O_{18}$ as the main mineral phase (Figure S1). In addition, CeO_2 and ZrO_2 were also found to be present in the catalyst. The identification of the PGM phases in this material by XRD is challenging because of the low total concentration of these elements (<0.25 wt %) and the complex composition of the wash coat, resulting in many overlapping X-ray reflections. Only small diffraction peaks of the PdO and PtO_2 phases could be detected. The EPMA analysis showed that the PGMs are randomly distributed throughout the whole catalyst structure (Figure S2). Furthermore, PGMs are present mostly together with Ce. The impurities Al, Si, Ce, Zr, Mg, and so forth represent the major composition of the cordierite and the wash coat in the honeycomb material of the catalyst. EPMA point analysis gave different values of the PGM

https://dx.doi.org/10.1021/acssuschemeng.0c07355
ACS Sustainable Chem. Eng. 2021, 9, 337−350

concentration because of the random distribution of these elements (Figure S3). Furthermore, the determination of Pt was problematic because the characteristic peak of Pt overlapped with an intense Zr peak. Therefore, microwave digestion followed by ICP−OES analysis was used for the quantitative characterization of the catalyst powder. The elemental composition is summarized in Table 1.

Table 1. Elemental Composition of the Spent Automotive Catalysts

element	concentration ± standard deviation (mg kg^{-1})
Pt	735 ± 15
Pd	1536 ± 30
Rh	269 ± 5
Al	188,001 ± 3760
Si	49,226 ± 2208
Mg	33,205 ± 351
Ce	30,442 ± 686
Zr	26,980 ± 250
Ca	2886 ± 58
Fe	5005 ± 335
Zn	2079 ± 12
Ni	233 ± 65
Cu	123 ± 2
Cr	260 ± 23
As	132 ± 4
Mn	185 ± 7
Pb	410 ± 5
Sc	59 ± 1
Co	12 ± 1

Solvoleaching of the Spent Automotive Catalysts. The leaching behavior of the PGMs was studied as a function of the temperature (*i.e.*, from 20 to 80 °C) in four organic lixiviants (*i.e.*, $CuCl_2/CH_3CN$, $CuCl_2$/DMSO, $FeCl_3/CH_3CN$, and $FeCl_3$/DMSO). The temperature was set below 80 °C to avoid (i) pressure buildup due to the low boiling point of CH_3CN (82 °C) and (ii) violent decomposition of DMSO in the presence of oxidants such as $CuCl_2$ and $FeCl_3$.[31] Other parameters were kept constant.

Figure 1 indicates that the leaching efficiency of palladium is temperature-dependent in all the investigated solvent systems. The dissolution of palladium increased significantly above 40 °C and reached a plateau at 70 °C. The extraction behavior of Pd in $FeCl_3/CH_3CN$ is quantitatively similar to the one in $CuCl_2/CH_3CN$ (Figure 1A,C). In both systems, maximum dissolution of 75% Pd was achieved at 70 °C. Furthermore, the percentage of Pd leached was higher in $CuCl_2$/DMSO than that in $FeCl_3$/DMSO, 75 and 37% at 70 °C, respectively. In contrast, the leaching efficiency of Pt and Rh is limited and remains almost constant as a function of the temperature in all the systems. When using $FeCl_3$/DMSO as a lixiviant, the leaching efficiencies of Pt (<0.3%) and Rh (<0.8%) were almost negligible. These results are consistent with those reported for "*organic aqua regia*" (*i.e.*, $SOCl_2$ in pyridine), in which Pd is easily dissolved, whereas Pt is not.[24] Considering this dissolution behavior of PGMs, further leaching experiments were carried out at 70 °C.

Figure 2 compares the effect of leaching time on the dissolution of PGMs in different systems. Up to 62% of Pd was leached in $CuCl_2/CH_3CN$ and 54% of Pd was leached in $FeCl_3/CH_3CN$ after 5 min. The leaching percentage of Pd

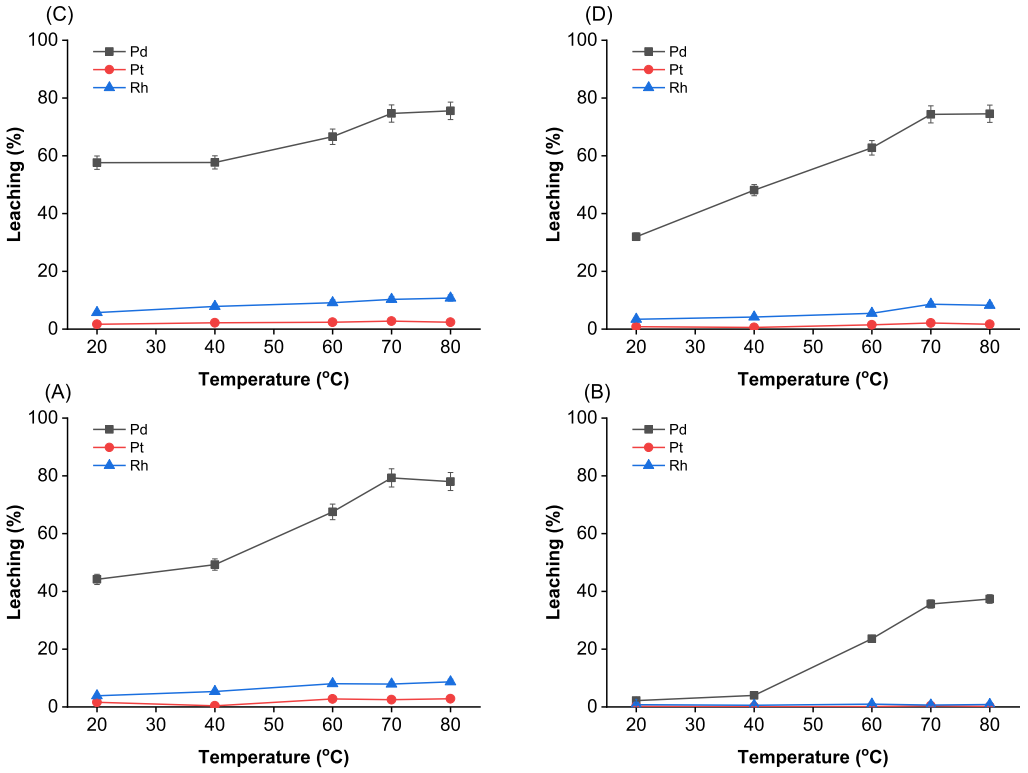

Figure 1. Effect of temperature on the dissolution of PGMs from spent automotive catalysts in (A) $FeCl_3/CH_3CN$, (B) $FeCl_3$/DMSO, (C) $CuCl_2/CH_3CN$, and (D) $CuCl_2$/DMSO as lixiviants. Temperature, 20−80 °C; stirring speed, 700 rpm; S/L ratio, 100 g L^{-1}; time, 120 min; and $FeCl_3$ and $CuCl_2$ concentration, 0.04 mol L^{-1}.

https://dx.doi.org/10.1021/acssuschemeng.0c07355
ACS Sustainable Chem. Eng. 2021, 9, 337−350

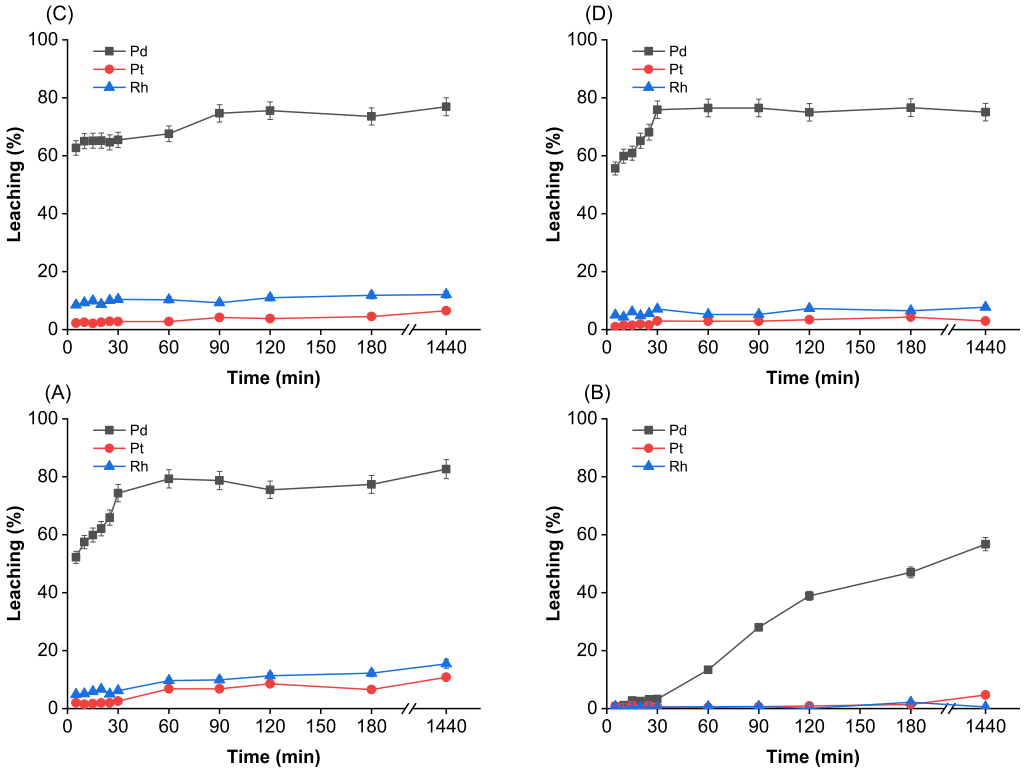

Figure 2. Effect of leaching time on the dissolution of PGMs from spent automotive catalysts in (A) $FeCl_3/CH_3CN$, (B) $FeCl_3$/DMSO, (C) $CuCl_2/CH_3CN$, and (D) $CuCl_2$/DMSO as lixiviants. Temperature, 70 °C; stirring speed, 700 rpm; S/L ratio, 100 g L^{-1}; time, 5−1440 min; and $FeCl_3$ and $CuCl_2$ concentration, 0.04 mol L^{-1}.

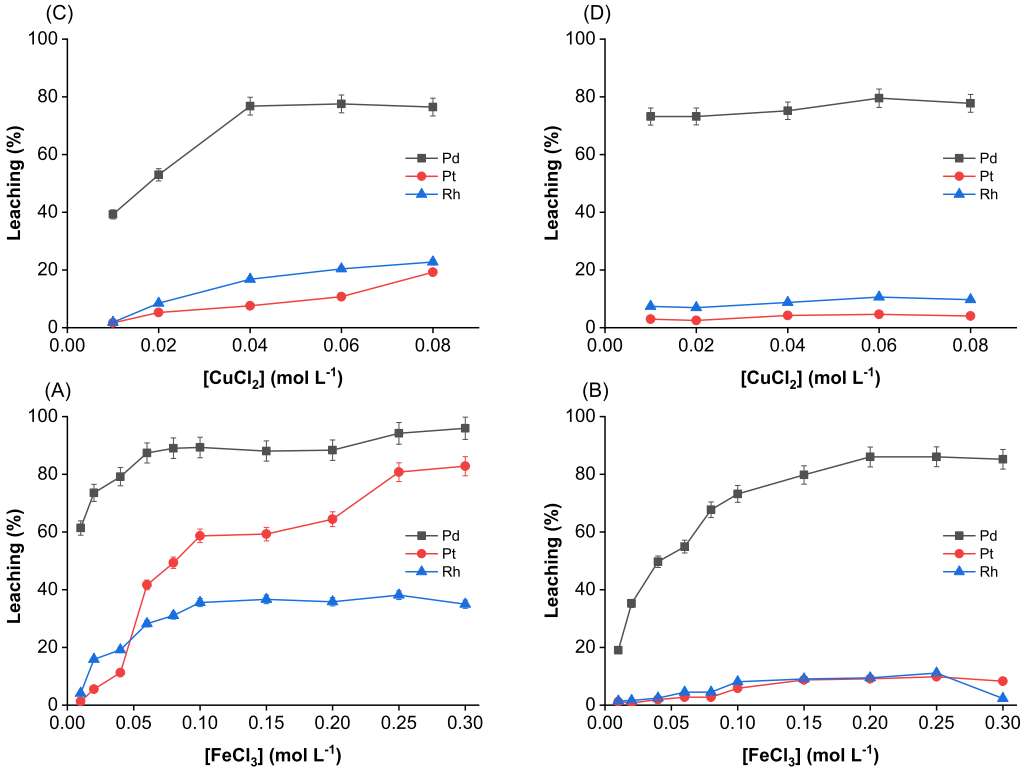

Figure 3. Effect of concentration of the oxidizing agent on the dissolution of PGMs from spent automotive catalysts in (A) $FeCl_3/CH_3CN$, (B) $FeCl_3$/DMSO, (C) $CuCl_2/CH_3CN$, and (D) $CuCl_2$/DMSO as lixiviants. Temperature, 70 °C; stirring speed, 700 rpm; S/L ratio, 100 g L^{-1}; time, 180 min; $FeCl_3$ concentration, 0.01−0.3 mol L^{-1}; and $CuCl_2$ concentration, 0.01−0.08 mol L^{-1}.

with $CuCl_2/CH_3CN$ remained quite constant (about 65%) from 5 to 30 min and moderately increases up to 78% at 90 min. Prolongation of the leaching time to more than 90 min resulted in a constant Pd extraction (ca. 78%), while Pt and Rh

https://dx.doi.org/10.1021/acssuschemeng.0c07355
ACS Sustainable Chem. Eng. 2021, 9, 337−350

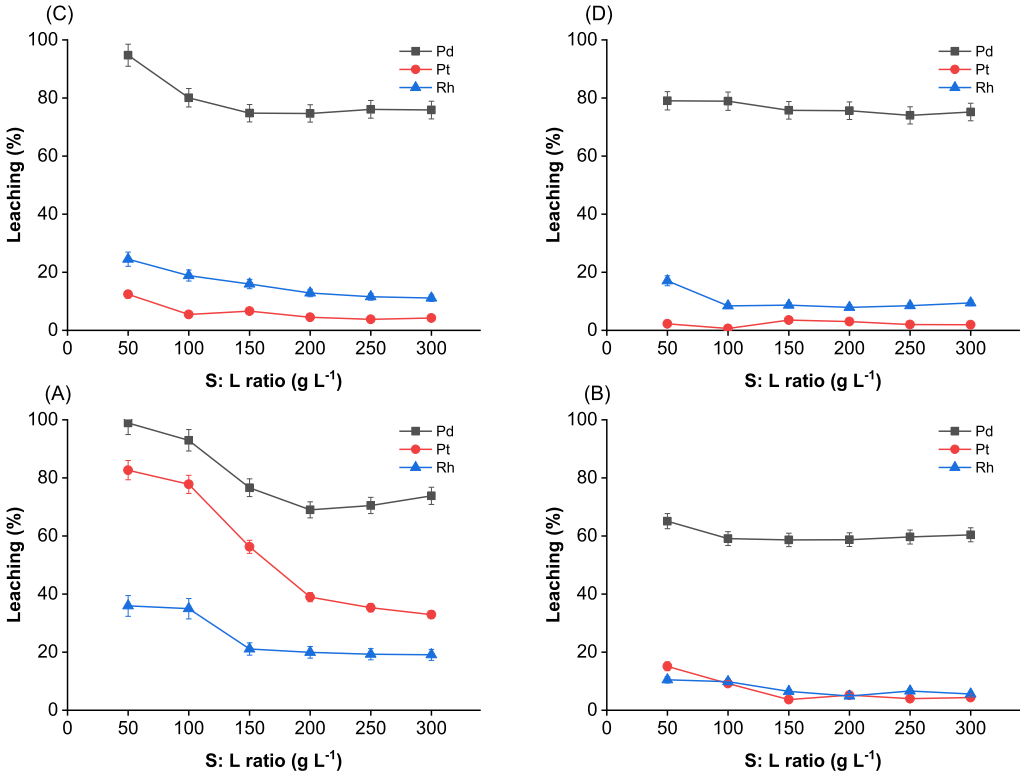

Figure 4. Effect of the S/L ratio on the dissolution of PGMs from spent automotive catalysts in (A) $FeCl_3/CH_3CN$, (B) $FeCl_3$/DMSO, (C) $CuCl_2/CH_3CN$, and (D) $CuCl_2$/DMSO as lixiviants. Temperature, 70 °C; stirring speed, 700 rpm; S/L ratio, 50−300 g L^{-1}; time, 180 min; $FeCl_3$ concentration, 0.3 mol L^{-1}; and $CuCl_2$ concentration, 0.08 mol L^{-1}.

remained largely in the residue (Figure 2C). On the other hand, up to 77% of Pd was dissolved in 30 min using $FeCl_3/CH_3CN$ and remained constant for longer leaching. Figure 2A,C shows that the equilibrium for Pd dissolution is reached slightly faster in $FeCl_3/CH_3CN$ than in $CuCl_2/CH_3CN$. In addition, less than 1% Pt and 3% Rh were dissolved in $FeCl_3/CH_3CN$ after 30 min of contact time. The negligible dissolution of Pt and Rh suggests that Pd can be selectively leached from spent automotive catalysts by adjusting the leaching time: the shorter the reaction time is, the higher the selectivity for the leaching of Pd.

Figure 2B,D shows the different leaching behaviors of PGMs in $FeCl_3$/DMSO and $CuCl_2$/DMSO as a function of time. The initial dissolution of Pd in $CuCl_2$/DMSO follows a similar trend to the dissolution in $FeCl_3/CH_3CN$ (Figure 2A). Equilibrium was reached after 30 min of leaching, when most of the Pd was leached (ca. 78%), while Pt and Rh remained in the residue. In contrast, the dissolution of PGMs in $FeCl_3$/DMSO was very slow. None of the PGMs were dissolved within 30 min. The leaching efficiency of Pd slightly increased from 16 to 59% when the contact time was increased from 60 to 1440 min. Negligible amounts of <0.5% Pt and Rh were dissolved in $FeCl_3$/DMSO, regardless of the contact time. Although the $FeCl_3$/DMSO system is the most selective for the leaching of Pd over Pt and Rh, the leaching rate is too slow to be of practical use. The leaching of Pd in $FeCl_3$/DMSO (Figure 2B) was significantly slower than that in $FeCl_3/CH_3CN$ (Figure 2A).

The next variable investigated was the effect of the concentration of the oxidizing agent. The $FeCl_3$ concentration was varied from 0.01 to 0.3 mol L^{-1} (Figure 3A,B); meanwhile, the $CuCl_2$ concentration was varied only between 0.01 and 0.08 mol L^{-1} because of its limited solubility in the organic solvents. Figure 3C,D shows the leaching behavior of PGMs with different concentrations of $CuCl_2$ in CH_3CN and DMSO, respectively. Higher concentrations of $CuCl_2$ resulted in higher leaching of PGMs in CH_3CN. The percentage of Pd leached increased from 40 to 78% when increasing the $CuCl_2$ concentration from 0.01 to 0.04 mol L^{-1}. The leaching efficiency of Pd remained stable with further increase in $CuCl_2$ concentration up to 0.08 mol L^{-1}. The percentage of Pt and Rh leached gradually increased from 0.5 to about 20% within the investigated range. On the other hand, the leaching of 76% Pd, 4.2% Pt, and 8.5% Rh in DMSO remained almost constant regardless of the variation in $CuCl_2$ concentration. The dissolution of Pt and Rh in $CuCl_2/CH_3CN$ is mostly higher than that in $CuCl_2$/DMSO. The reason is that Cu^{2+} is a stronger oxidizing agent in CH_3CN ($E°$ Cu^{2+}/Cu^{+} = +1.21 V) than in DMSO ($E°$ Cu^{2+}/Cu^{+} = +0.31 V).[32−35]

The dissolution of PGMs using different $FeCl_3$ concentrations in CH_3CN and DMSO was also studied (Figure 3A,B). In DMSO, the leaching efficiency of Pd substantially increased with increasing $FeCl_3$ concentration. Figure 3B shows that a maximum of 82% Pd was leached along with less than 10% codissolution of Rh and Pt using 0.2−0.3 mol L^{-1} $FeCl_3$/DMSO. On the other hand, the leaching efficiency of Pd, Pt, and Rh increased when using the same $FeCl_3$ concentration in CH_3CN. This can be attributed to the lower formal reduction potential of the Fe^{3+}/Fe^{2+} couple in DMSO ($E°$ = +0.21 V) compared to that in CH_3CN ($E°$ = +1.57 V).[32,34] As shown in Figure 3A, more PGMs were dissolved using higher $FeCl_3$ concentrations. For instance, a concentration of 0.01 mol L^{-1} $FeCl_3$ allowed the selective leaching of 62% Pd, with only 0.2% Pt and 4% Rh

https://dx.doi.org/10.1021/acssuschemeng.0c07355
ACS Sustainable Chem. Eng. 2021, 9, 337−350

codissolution. At the same time, up to 90% Pd, together with 80% Pt, and 35% Rh were leached using 0.3 mol L^{-1} $FeCl_3$/CH_3CN. These results indicate that it is possible to tune the selectivity by only changing the $FeCl_3$ concentration.

The dependence PGM leaching efficiency on the variation in the solid-to-liquid ratio (S/L) was determined. Figure 4 shows that increasing the S/L ratio from 50 to 300 g L^{-1} led to a different extent of decrease in percentage extraction of PGMs in all systems. The leaching of PGMs in $FeCl_3$/DMSO and $CuCl_2$/DMSO slightly decreased when increasing the S/L ratio (Figure 4B,D). On the other hand, varying the S/L ratio had a pronounced effect on the leaching of PGMs in CH_3CN. As shown in Figure 4A,C, Pd was completely leached at a S/L of 50 g L^{-1} in both $FeCl_3$/CH_3CN and $CuCl_2$/CH_3CN systems. A significant decrease in leaching efficiency of Pd was observed when increasing the S/L ratio from 50 to 300 g L^{-1} in CH_3CN. The dissolution of Pt and Rh in $CuCl_2$/CH_3CN was found to be less dependent on the S/L ratio than that in $FeCl_3$/CH_3CN. The leaching efficiency decreased from 16 to 3% for Pt and 22% to 18% for Rh using $CuCl_2$/CH_3CN in the range of investigated S/L ratios. Meanwhile, up to 80−82% Pt and 38−40% Rh were dissolved when using $FeCl_3$/CH_3CN at 50−100 g L^{-1} S/L. Taking into account the leaching efficiency and the final concentration of PGMs in the leachate, a S/L ratio of 100 mg L^{-1} was chosen for further experiments.

It is important to select lixiviants that allow not only the dissolution of the PGMs but are also compatible with the subsequent NASX step for separation of the PGMs into the individual elements. Figure 5 shows that Pd can be dissolved in

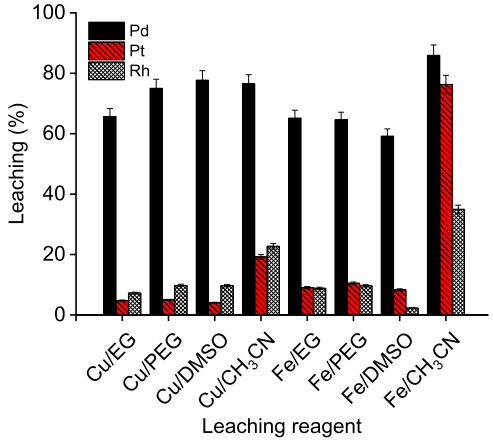

Figure 5. Dissolution of PGMs from the spent automotive catalyst powder using different lixiviants under optimized conditions. Conditions: 70 °C, 700 rpm, S/L ratio: 100 g L^{-1}, 180 min, 0.3 mol L^{-1} $FeCl_3$ or 0.08 mol L^{-1} $CuCl_2$ in DMSO, CH_3CN, EG, and PEG.

all the investigated solvent systems. The leaching efficiency of Pd increased according to the following sequence: $FeCl_3$/DMSO < $FeCl_3$/EG ≈ $FeCl_3$/PEG ≈ $CuCl_2$/EG < $CuCl_2$/PEG ≈ $CuCl_2$/DMSO ≈ $CuCl_2$/CH_3CN < $FeCl_3$/CH_3CN. The codissolution of Pt and Rh is limited when using $CuCl_2$/EG, Cu^{2+}/PEG, $CuCl_2$/DMSO, $FeCl_3$/EG, $FeCl_3$/PEG, and $FeCl_3$/DMSO. The highest leaching percentage of Pt (76%) and Rh (38%) was achieved using $FeCl_3$/CH_3CN. Therefore, the $FeCl_3$/CH_3CN was selected as the best system because it allowed either the selective leaching of Pd or the complete extraction of all PGMs by varying the $FeCl_3$ concentration. The main drawback of using CH_3CN is that it is miscible with most of the conventional diluents used in solvent extraction. However, CH_3CN can be easily distilled and recovered prior to solvent extraction, followed by redissolution of the solid residue in another polar solvent that is compatible with NASX. Additionally, the process based on $FeCl_3$/CH_3CN is versatile, which allows either selective leaching of Pd or complete leaching of PGMs. In this study, the selective dissolution of PGMs was preferred, as it facilitates the further separation of PGMs.

Solution Chemistry and Mechanism for Solvoleaching of PGMs. The results presented in the previous section suggest that the factors influencing the dissolution of PGMs in organic solvents are (i) solvation of metal ions, (ii) reduction potential of the Fe^{3+}/Fe^{2+} and Cu^{2+}/Cu^{+} redox couples, (iii) temperature, (iv) leaching time, and (v) oxidizing agent concentration.

In a comparative study, the dissolution of PGMs from the spent automotive catalysts was investigated using an aqueous solution of 0.3 mol L^{-1} Fe^{3+}/H_2O and 0.04 mol L^{-1} Cu^{2+}/H_2O at an optimized temperature of 70 °C. Unlike the solvoleaching systems, the leaching efficiency of PGMs, more particularly of Pd, was negligible (<2%) in the aqueous systems. The limited dissolution of Pd in the aqueous systems can be explained by hard and soft acid and base (HSAB) theory. Hard Lewis acids tend to interact strongly with hard Lewis bases, while soft Lewis acids interact strongly with soft bases. In the aqueous leaching system, water is a hard oxygen donor solvent, which solvates hard acceptors fairy well (*i.e.*, Fe^{3+}, Al^{3+}, H^{+}...) but soft acceptors poorly (*i.e.*, Pd^{2+}, Pt^{2+}, Au^{+}, Ag^{+}, and Cu^{+}) via electrostatic interactions.[33] The nature of the donor atom strongly affects the stability of the metal complex. DMSO is an aprotic solvent, which usually coordinates through its oxygen atom, but it solvates the most soft metal ions such as Pd(II) and Pt(II) ions via its sulfur atom, for example, [Pd-$(DMSO)_2Cl_2$].[36] The halo complexes of Cu(I) are more stable in dipolar aprotic solvents such as DMSO than in water because the large polarizable complex ions $CuCl_2^-$ are well solvated and readily form $Cu(DMSO)_2Cl_2$. On the other hand, CH_3CN is an aprotic nitrogen donor solvent with a soft electron pair donor, solvating the monovalent d^{10} metal ions Cu(I), Ag(I), and Au(I) especially well. In fact, the Cu(I) ion is a fairly soft electron pair acceptor, while the Cu(II) ion is a borderline one. Because Cu(I) is more strongly solvated than Cu(II), the cuprous form is more stable in soft donor solvents such as CH_3CN than in water.[33]

The PGM complex formation in the organic solvents CH_3CN and DMSO was characterized by FTIR and UV−vis spectroscopy. For palladium complex formation, Figure 6A shows that the C−N stretching frequency for acetonitrile (ν_{C-N} 2266 cm^{-1}) increases to 2331 cm^{-1}, while ν_{C-C} increases from 920 to 950 cm^{-1}. In fact, acetonitrile coordination strengthens the C−N and C−C σ bonding, which causes increased force constants. The result reveals that the coordination of Pd(II) and acetonitrile through nitrogen suggests a formation of relatively strong Pd−ligand bonding in the square-planar neutral complex $[Pd(CH_3CN)_2Cl_2]$. Besides, the interpretation is also consistent with the UV−vis absorption spectra, as shown in Figure 6C. The square-planar coordination geometry of $[Pd(CH_3CN)_2Cl_2]$ complexes, in which the central palladium atom coordinates two nitrogen atoms of CH_3CN ligands and two chlorine atoms, was manifested by two absorption bands at 300−400 nm, corresponding to metal−ligand charge transfer transitions.

https://dx.doi.org/10.1021/acssuschemeng.0c07355
ACS Sustainable Chem. Eng. 2021, 9, 337−350

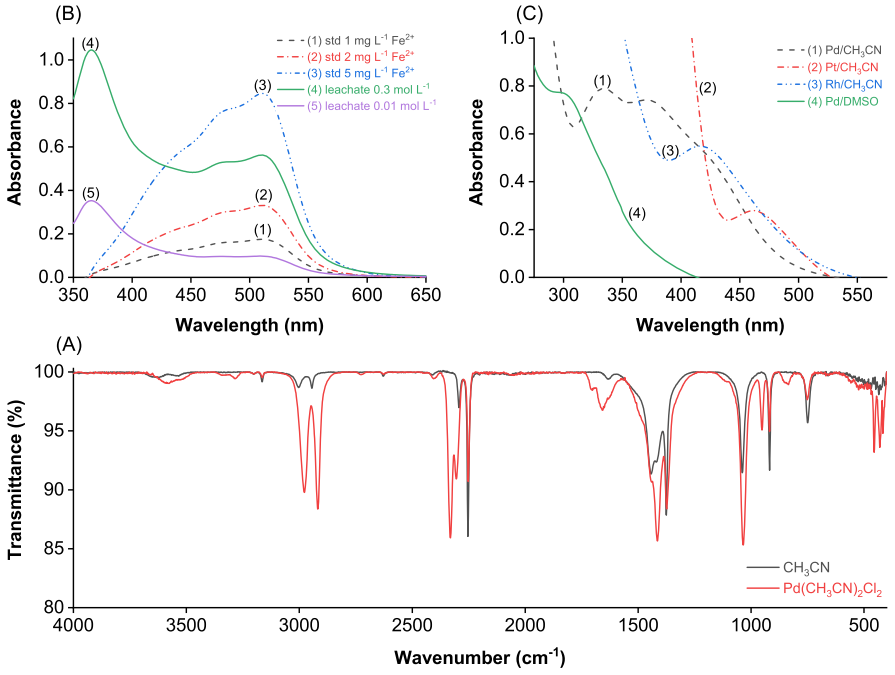

Figure 6. (A) FTIR spectra of Pd(II) complexes in CH_3CN; (B) UV−vis absorption spectra of the Fe(II) standard solutions and the Fe(II) formed after the dissolution of the spent automotive catalysts with 0.3 mol L^{-1} and 0.01 mol L^{-1} $FeCl_3/CH_3CN$; and (C) UV−vis absorption spectra of 0.3 g L^{-1} PGM complexes in CH_3CN and DMSO.

With regard to the complexes in DMSO, the FTIR spectra provided useful information about the coordination of PGMs with the sulfur donor site (Figure S10). The bands at 1134 and 1173 cm^{-1} assigned to ν_{S-O} (sulfur-bonded) indicate the formation of the neutral complexes $[Pd(DMSO)_2Cl_2]$ and $[Pt(DMSO)_2Cl_2]$, respectively. These findings about the general structural features of the neutral complexes of PGMs in organic solvents, $[ML_2Cl_2]$ (L = CH_3CN or DMSO), are in line with the ones reported in the literature.[36,37]

Taking into account the metal complex formation in the organic solvents, the leaching reaction mechanism for dissolution of PGMs can be proposed as

$$n[FeL_2Cl_3]^{3+} + M^0 \leftrightarrows n[FeLCl_2]^{2+} + [ML_nCl_n]^{n+} \quad (4)$$

$$n[CuL_2Cl_2]^{2+} + M^0 \leftrightarrows n[CuLCl]^{+} + [ML_nCl_n]^{n+} \quad (5)$$

where L = CH_3CN or DMSO and M = Pd, Pt, and Rh with n = 2, 2, and 3, respectively.

To support the proposed mechanism, the oxidation state of iron was examined in the pregnant leach solutions $FeCl_3/CH_3CN$ using UV−vis absorption spectroscopy. The presence of Fe(II) cations after leaching was established using a chelating colorimetric agent, 1, 10-phenanthroline (phen). As shown in Figure 6B, the absorption maximum at λ_{max} = 511 nm in an acidic aqueous solution (pH = 3.5) confirms the presence of the orange complex $[Fe(phen)_3]^{2+}$. The concentration of Fe(II) was further measured in two leachates generated after the leaching of spent automotive catalysts using 0.01 and 0.3 mol L^{-1} $FeCl_3/CH_3CN$. The former and latter leachate contained 180 and 3300 mg L^{-1} Fe(II), respectively. The higher the concentration of Fe(III) used to leach, the higher the leaching of PGMs and therefore the more the Fe(II) formed. When 0.01 mol L^{-1} $FeCl_3/CH_3CN$ was used, the molar ratio of Fe(II) formed in the leachate (3.21 mmol L^{-1}) is twofold higher than that of Pd^{2+} (1.41 mmol L^{-1}) dissolved in 0.01 mol L^{-1} $FeCl_3/CH_3CN$. The result suggests that the stoichiometry of Pd(II)/Fe(II) is 1:2, as expressed in eq 4.

Next, the effects of the solvent on the redox potentials and the reaction mechanism were considered. Table 2 summarizes

Table 2. Formal Reduction Potentials of Iron and Copper Redox Couples in Water, CH_3CN, and DMSO at 25 °C

redox couple	reduction half-reaction	formal reduction potential ($E°$, V) H_2O	CH_3CN	DMSO	references
Cu^{2+}/Cu^+	$Cu^{2+} + e^- \rightarrow Cu^+$	+0.16	+1.21	+0.31	33,35
			+0.92	+0.50	38,39
Fe^{3+}/Fe^{2+}	$Fe^{3+} + e^- \rightarrow Fe^{2+}$	+0.77	+1.57	+0.21	32,40
			+1.36	+0.14	

the formal reduction potentials of Fe^{3+}/Fe^{2+} and Cu^{2+}/Cu^+ in water, CH_3CN, and DMSO. The reduction potential of Cu^{2+} is less positive in water than that in DMSO and CH_3CN (Table 2). As a result, Cu^{2+} is a relatively mild oxidizing agent in both dipolar aprotic organic solvents. In general, because of its lower charge density, Cu^+ is better stabilized in solvents with lower dielectric constants: (ε_{H_2O} = 78.5) > (ε_{DMSO} = 46.7) > (ε_{CH_3CN} = 37.5). Similarly, the formal reduction potential of the Fe^{3+}/Fe^{2+} couple in CH_3CN is estimated to be +1.57 V (Table 2). The high formal potential indicates that Fe^{3+} is an effective and powerful oxidant in CH_3CN. The significant increase in the reduction potential of the Fe^{3+}/Fe^{2+} couple in CH_3CN is partly attributed to the low dielectric constant of CH_3CN, which promotes ion association.

To further support the proposed reaction mechanism, the formal reduction potentials of the Fe^{3+}/Fe^{2+} and Cu^{2+}/Cu^+ couples in DMSO and CH_3CN were investigated. CVs of the blank electrolyte, DMSO, and CH_3CN were recorded to determine the electrochemical window (Figure S4). Next, the

https://dx.doi.org/10.1021/acssuschemeng.0c07355
ACS Sustainable Chem. Eng. 2021, 9, 337−350

electrochemical behavior of copper and iron in DMSO and CH_3CN was studied to determine the formal reduction potentials of the Fe^{3+}/Fe^{2+} and Cu^{2+}/Cu^{+} redox couples (Figures S5–S8). The interpretation of all the CVs recorded is available in the Supporting Information. The systems however have proven to be more complex than expected at first glance. We assume that several Cu(II) acetonitrile and Fe(III) acetonitrile/DMSO complexes are present in solution, making it very difficult to measure the formal redox potentials. However, it is possible to draw some conclusions from these CVs regarding the oxidative power of both metals. When comparing the cathodic peak potentials (E_{pc}) of the Fe^{3+}/Fe^{2+} and Cu^{2+}/Cu^{+} couples as assigned on the CVs, it is clear that the E_{pc} is more positive in CH_3CN than in DMSO (Table 3).

Table 3. Cathodic Peak Potentials of Fe^{3+}/Fe^{2+} and Cu^{2+}/Cu^{+} Redox Couples in CH_3CN and DMSO[a]

		cathodic peak potentials (E_{pc}, V)	
redox couples	reduction half-reaction	DMSO	CH_3CN
Cu^{2+}/Cu^{+}	$Cu^{2+} + e^- \rightarrow Cu^{+}$	−0.74	+0.33
			−0.03
Fe^{3+}/Fe^{2+}	$Fe^{3+} + e^- \rightarrow Fe^{2+}$	−0.63	+0.42
		−1.27	−0.34

[a]Assigned based on the CVs recorded on a GC electrode at room temperature at a scan rate of 100 mV s^{-1}.

This shows that the Fe(II) and Cu(I) chloro complex species are better stabilized in CH_3CN than in DMSO. Also, the E_{pc} for the Fe^{3+}/Fe^{2+} redox couple is more positive than that for the Cu^{2+}/Cu^{+} redox couple in the same solvent, leading to the conclusion that Fe(II) chloro acetonitrile complex species are more stabilized than the Cu(I) chloro acetonitrile complex species. Although the formal potential is difficult to determine, based on the E_{pc}, it is assumed that Fe(III) is a stronger oxidizing agent than Cu(II).

There is a great difference in the leaching behavior of platinum in the $FeCl_3/CH_3CN$ and $CuCl_2/CH_3CN$ system (Figure 3). Only a small amount of platinum was leached in the 0.08 mol L^{-1} $CuCl_2/CH_3CN$ system (% L = 19%) compared to in the 0.08 mol L^{-1} $FeCl_3/CH_3CN$ system (% L = 50%). This can be explained by the corrosion current in both systems. Polarization curves were recorded on a platinum electrode, in a potential range of ±600 mV with respect to the OCP for the 0.08 mol L^{-1} $FeCl_3/CH_3CN$ system and in a potential range of−600 till +1000 mV with respect to the OCP for the 0.08 mol L^{-1} $CuCl_2/CH_3CN$ system, at a scan rate of 1 mV/s (Figure 7). The linear Tafel region was determined from piecewise linear regression analysis.[41]

The corrosion potential of platinum in the 0.08 mol L^{-1} $FeCl_3/CH_3CN$ system (E_{corr} = +1.19 V) is more positive than that for the 0.08 mol L^{-1} $CuCl_2/CH_3CN$ system (E_{corr} = +0.99 V), indicating that the driving force for the corrosion of platinum is larger in the 0.08 mol L^{-1} $FeCl_3/CH_3CN$ system than in the 0.08 mol L^{-1} $CuCl_2/CH_3CN$ system. This validates the observations during leaching. The corrosion potential of the 0.08 mol L^{-1} $CuCl_2/CH_3CN$ system is at a higher potential than the OCP. An overpotential is needed to corrode platinum. The anodic wave starting at the OCP until 0.9 V versus Ag^{+}/Ag is a consequence of Cu(I) to Cu(II) oxidation. Probably some Cu(I) is always in equilibrium with Cu(II) in the solution because of the high stability of Cu(I) in

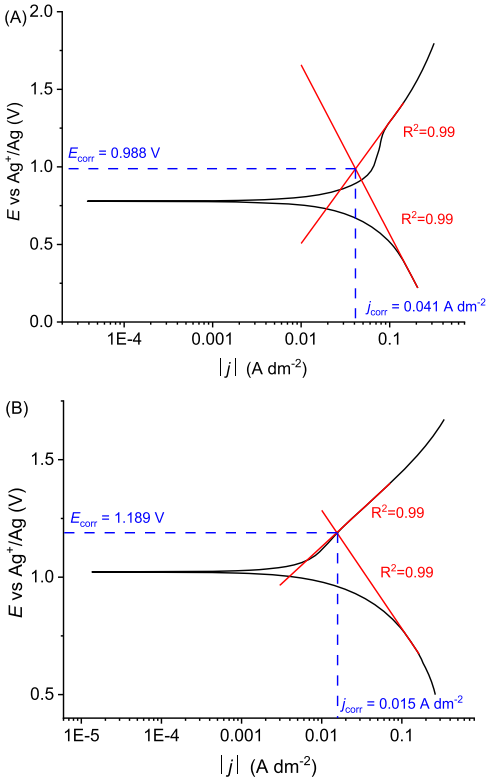

Figure 7. Polarization curves recorded on a platinum electrode at a scan rate of 1 mV/s for the 0.08 mol L^{-1} $CuCl_2/CH_3CN$ (A) in a potential range of−600 till +1000 mV with respect to the OCP and 0.08 mol L^{-1} $FeCl_3/CH_3CN$ (B) system in a potential range of ±600 mV with respect to the OCP.

acetonitrile. This complicates the prediction of the corrosion potential and current. It is not expected that the corrosion potential deviates greatly from the OCP. The corrosion potential of the 0.08 mol L^{-1} $FeCl_3/CH_3CN$ system is only slight above the OCP, showing that platinum corrosion occurs at the OCP.

Besides polarization curves, chronoamperometric measurements were conducted at the OCP for 30 min on a Pt electrode for the blank electrolyte (CH_3CN), 0.08 mol L^{-1} $CuCl_2/CH_3CN$, and 0.3 mol L^{-1} $FeCl_3/CH_3CN$ system (Figure 8). After 30 min, the current density in the 0.3 mol L^{-1} $FeCl_3/CH_3CN$ system is almost 40 times bigger than that in the 0.08 mol L^{-1} $CuCl_2/CH_3CN$ system. The low current

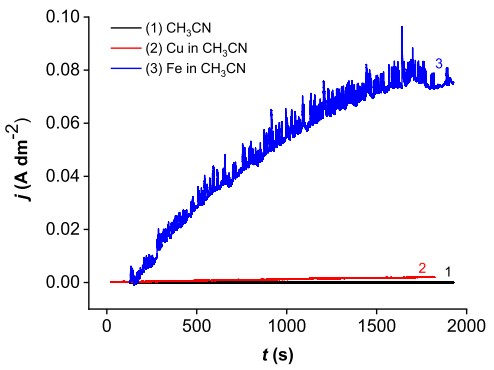

Figure 8. Chronoamperometric curves recorded on a Pt electrode for 30 min at the OCP for the blank electrolyte, (1) CH_3CN, (2) 0.08 mol L^{-1} $CuCl_2/CH_3CN$, and (3) 0.3 mol L^{-1} $FeCl_3/CH_3CN$.

https://dx.doi.org/10.1021/acssuschemeng.0c07355
ACS Sustainable Chem. Eng. 2021, 9, 337−350

density is a direct consequence of the limited dissolution of $CuCl_2$ in acetonitrile compared to $FeCl_3$. The combination of the lower E_{corr} and the very low current density explains why the leaching percentage of platinum (OCP) in the 0.08 mol L^{-1} $CuCl_2/CH_3CN$ system is much smaller compared to that in the 0.3 mol L^{-1} $FeCl_3/CH_3CN$ system.

Upscaling Solvoleaching of PGMs. Selective leaching of Pd was performed at a larger scale in which 10 g of spent automotive catalysts was dissolved in 100 mL of 0.01 mol L^{-1} $FeCl_3/CH_3CN$ at 70 °C. The reactor was equipped with a reflux condenser, a dropping funnel, and a magnetic stirrer. The three consecutive leaching steps were carried out to recover Pd as much as possible. Table 4 shows that a total of up to 95.2% Pd was dissolved with codissolution of only 1.22% Pt and 5.17% Rh in the multistage leaching. The Pd leachate solutions from the different steps were mixed and the CH_3CN was recovered by distillation. Next, the residue that was obtained after selectively leaching the Pd (and that was rich in Pt and Rh) was leached with 0.3 mol L^{-1} $FeCl_3/CH_3CN$. Up to 82.5% Pt and 38.9% Rh were extracted in a single leaching step. Table 4 indicates a total recovery of 97.7% Pd, 83.7% Pt, and 44.1% Rh. The lower leaching efficiency of Rh can be attributed to the more refractory nature of the Rh_2O_3 oxide film in the spent automotive catalysts.[9]

Table 4. Multistage Selective Dissolution of PGMs from the Automotive Catalyst Powder[a]

	leaching percentage (%)				
	0.01 mol L^{-1} $FeCl_3/CH_3CN$			0.3 mol L^{-1} $FeCl_3/CH_3CN$	
elements	1st stage	2nd stage	3rd stage	1st stage[b]	total[c]
Pd	62.1	29.6	3.45	2.55	97.7
Pt	1.02	0.16	0.04	82.5	83.7
Rh	4.23	0.35	0.59	38.9	44.1
Al	0.00	0.01	0.02	0.60	0.63
Si	0.00	0.00	0.00	0.03	0.04
Mg	0.16	0.05	0.04	0.42	0.66
Ce	0.01	0.07	0.04	1.50	1.61
Zr	0.00	0.01	0.01	0.24	0.26
Ca	5.85	4.80	4.41	14.7	29.8
Fe					
Zn	1.62	2.69	1.48	5.88	11.7
Ni	8.29	4.39	2.83	19.9	35.4
Cu	22.3	4.87	3.10	17.8	48.1
Cr	10.0	7.18	4.03	21.8	43.0
As	6.42	0.27	2.94	1.81	11.4
Mn	31.3	28.1	27.7	13.1	100.2
Pb	0.97	1.42	3.21	13.9	19.5
Sc	0.01	0.01	0.17	5.16	5.4
Co	37.3	9.01	10.5	43.2	100.0

[a]Conditions: 70 °C, 700 rpm, S/L ratio: 100 g L^{-1}, 30 min with 0.01 mol L^{-1} $FeCl_3/CH_3CN$ (three stages), and 180 min with 0.3 mol L^{-1} $FeCl_3$ in CH_3CN. [b]Leaching efficiency calculated for the solid residue remaining after 3-stage selective leaching of Pd with 0.01 mol L^{-1} $FeCl_3/CH_3CN$. [c]Cumulative leaching efficiency of PGMs after 4-stage leaching (three stages for selective Pd leaching and one stage for Pt and Rh leaching).

It is worth noting that the dissolution of metals present in cordierite $Mg_2Al_4Si_5O_{18}$ is negligible (<1%), even when 0.3 mol L^{-1} $FeCl_3/CH_3CN$ was used. This could be attributed to the refractory phases of cordierite and γ-alumina, whose dissolutions generally require strong acids. On the other hand, other impurities such as Ca, Zn, Ni, Cu, and Cr were moderately dissolved (30−50%), while complete dissolution of Mn and Co was achieved after multistage leaching with $FeCl_3/CH_3CN$. The presence of the impurities in the pregnant leaching solution at low concentrations, however, can be easily removed in a further NASX step. Obviously, the solvoleaching with $FeCl_3/CH_3CN$ allows highly selective dissolution of PGMs over cordierite. As a result, the process avoids the formation of silica gel during the conventional leaching of PGMs from spent automotive catalysts with strong acids. The solvent CH_3CN was also recovered by distillation and the solid residue remaining after the distillation step was redissolved in different polar solvents (*i.e.*, EG and DMSO) to further purify Pt and Rh by NASX.

Nonaqueous Solvent Extraction of PGMs. Direct solvent extraction from the CH_3CN-based leachates could not be performed because of the mutual miscibility of both phases when using extractants (*i.e.*, [A336][Cl], [P66614][Cl], TBP, Cyanex 923, TOA, and LIX 984) diluted in *p*-cymene. Therefore, CH_3CN was removed from the leachates by distillation. Subsequently, the residue containing Pt and Rh solid salts was redissolved in other polar solvents (DMSO or EG). These solvents are less harmful than the highly corrosive acidic HCl/Cl_2 solutions, which are widely used for dissolution of PGMs.

NASX of Pt and Rh from different polar feed solutions (DMSO or EG) was performed. Figure 9 compares the extraction behavior of PGMs and iron with different extractants, that is, [A336][Cl], [P66614][Cl], TBP, Cyanex 923, TOA, and LIX 984. The extraction of Fe(III) was also considered because it is the main impurity present in the leachate.

In DMSO, Pt(IV) was completely extracted using [P66614][Cl] with 80% Fe(III) and 35% Rh(III) coextraction (Figure 9B). On the other hand, the extraction of Pt(IV) was only 30% using [A336][Cl] because the mutual miscibility of [A336][Cl] is higher than that of [P666][Cl] with DMSO. The use of LIX 984 allowed the extraction of 60% Pt(IV), 58% Rh(III), and 44% Fe(III), but the phase separation was problematic because of formation of a stable emulsion. The extraction of Pt(IV) and Rh(III) was negligible (<10%) when using other extractants such as TBP, Cyanex 923, and TOA.

In EG, almost quantitative extraction of Pt(IV) and Fe(III) was achieved using [P66614][Cl], [A336][Cl], and TOA (Figure 9A). Both the ionic liquids [P66614][Cl] and [A336][Cl] allowed the selective extraction of Pt(IV) with <0.6 mg L^{-1} Rh(III) coextraction. The use of Cyanex 923 and LIX984 resulted in percentages of extraction of Pt(IV) between 22% and 38% and poor phase disengagement. Meanwhile, the extraction of PGMs with TBP was negligible (<5%). Taking into account the higher selectivity, [P66614][Cl] and [A336][Cl] were selected as extractants for further experiments.

The stripping of individual metals from loaded [P66614][Cl] and [A336][Cl] in *p*-cymene was investigated using different stripping agents (*i.e.*, thiourea, $NH_{3(aq)}$, $Na_2S_2O_3$, and H_2O), as shown in Figure S9 and Table 5.

The stripping of Pt(IV) from loaded [A336][Cl] was easier than that from loaded [P66614][Cl]. The complete stripping of Pt(IV) from the loaded [A336][Cl] was performed using either thiourea solution, aqueous NH_3, or $Na_2S_2O_3$. The use of

https://dx.doi.org/10.1021/acssuschemeng.0c07355
ACS Sustainable Chem. Eng. 2021, 9, 337−350

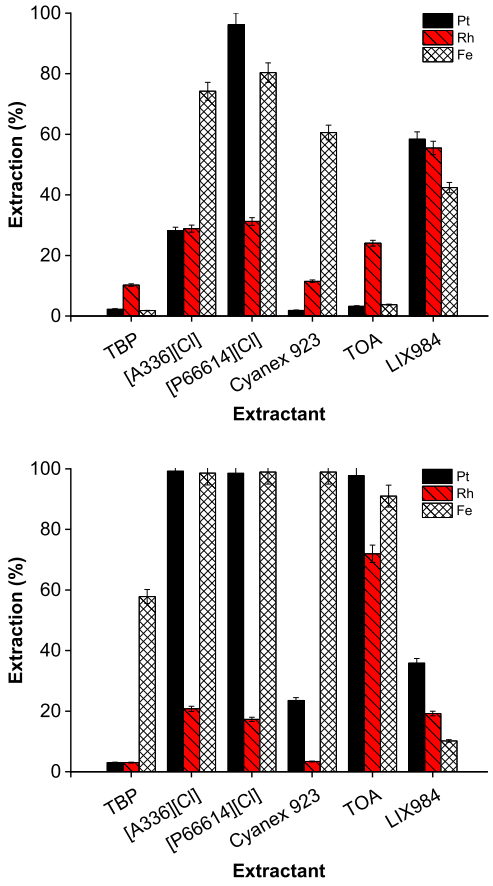

Figure 9. Nonaqueous solvent extraction of PGMs from (A) EG and (B) DMSO. Less-polar phase: 1.0 mol L^{-1} extractant in *p*-cymene; more polar phase: 36.9 mg L^{-1} Pt, 3.42 mg L^{-1} Rh, 12.3 g L^{-1} Fe; O/A = 1; 25 °C; and 60 min, 2000 rpm.

Table 5. Stripping of PGMs from the Loaded Organic Phases [P66614][Cl] and [A336][Cl] Using Water and Thiourea[a]

		percentage stripping (%)			
		polar feed DMSO		polar feed EG	
loaded organic	ions	H_2O	thiourea	H_2O	thiourea
[P66614][Cl]	Pt(IV)	<0.01[b]	5.15[b]	<0.01[d]	8.6[d]
	Rh(III)	<0.01[b]	<0.01[b]	<0.01[d]	<0.01[d]
	Fe(III)	20.4[b]	41.5[b]	20.9[d]	32.1[d]
[A336][Cl]	Pt(IV)	<0.01[c]	100[c]	<0.01[e]	100[e]
	Rh(III)	<0.01[c]	4.02[c]	<0.01[e]	<0.01[e]
	Fe(III)	55.8[c]	100[c]	75.4[e]	70.3[e]

[a]Conditions: 1.0 M thiourea; O/A = 1; 25 °C; and 60 min, 2000 rpm. [b]Loaded organic [P66614][Cl] 34.4 mg L^{-1} Pt, 1.21 mg L^{-1} Rh, 9.06 g L^{-1} Fe. [c]Loaded organic [A336][Cl] 5.4 mg L^{-1} Pt, 1.51 mg L^{-1} Rh, 8.45 g L^{-1} Fe from the polar feed in DMSO. [d]Loaded organic [P66614][Cl]. [e]Loaded organic [A336][Cl] 36.9 mg L^{-1} Pt, 0.68 mg L^{-1} Rh, 12.3 g L^{-1} Fe from the polar feed in EG.

$Na_2S_2O_3$, however, worsened the phase disengagement. Meanwhile, the stripping was problematic using aqueous NH_3 because of the precipitation of $Fe(OH)_3$. Therefore, water and the thiourea solution were chosen as the most promising stripping agents. Table 5 compares the stripping behavior of Fe(III) and Pt(IV) from loaded organic phases [P66614][Cl] and [A336][Cl] prepared from the polar feed DMSO and EG. The loaded [A336][Cl] from the EG feed is more preferred than that from DMSO because it allowed >75% Fe(III) scrubbing with water in a single contact. It is expected that no more than two stages are required for the complete removal of Fe(III). In addition, the complete stripping of Pt(IV) was only possible from loaded [A336][Cl] using a thiourea solution.

Conceptual Flow Sheet for PGM Recovery from Spent Automotive Catalysts. Based on the abovementioned experimental results, a conceptual flow sheet for a closed-loop process for the sustainable recovery of PGMs from spent automotive catalysts is proposed (Figure 10). The integrated process comprises two steps of solvoleaching, followed by NASX. First, Pd can be selectively leached using a solution of 0.01 mol L^{-1} $FeCl_3$ in CH_3CN. The leachate is distilled to recover CH_3CN. The Pd-containing residue is dissolved in water, from which Pd sponge can be produced by reduction with formic acid. Second, the residue from the leaching, which contains mainly Pt and Rh, can be further leached with 0.3 mol L^{-1} $FeCl_3$ in CH_3CN. The solvent CH_3CN is also recovered by distillation. The remaining solid after the distillation (Fe, Pt, and Rh) was redissolved in EG for further purification by NASX. Third, Pt(IV) and Fe(III) are selectively extracted with the ionic liquid [A336][Cl] while leaving Rh(III) in the raffinate. Next, Fe(III) is scrubbed with water. The quantitative stripping of Pt(IV) is achieved using a thiourea solution. Finally, the metal-free ionic liquid can be regenerated and reused.

The solvometallurgical process makes valuable contribution to the sustainable recovery of PGMs from spent automotive catalysts using less-harmful chemicals as compared to those of hydrometallurgical ones. The dissolution of PGMs with $FeCl_3$/CH_3CN is highly selective and environmentally friendly. The use of high temperatures and pressures or aggressive acidic leaching media (*i.e.*, Cl_2, HNO_3, or H_2O_2 in 6 mol L^{-1} HCl) is avoided. The solvent CH_3CN is easily recovered after leaching. Further purification of PGMs is straightforward. The reduction of Pd(II) with formic acid not only provides the high recovery of 99% Pd but also generates H_2O and CO_2 as products instead of H_2 gas when traditional cementation using granular Al or Zn is used. In addition, NASX with [A336][Cl] allows the complete separation of individual PGMs and Fe(III) in a safe and simply way. The recovery of Fe(III) with water avoids the use of basic solutions (*i.e.*, NaOH, $Ca(OH)_2$, and NH_4OH) for $Fe(OH)_3$ precipitation, which causes losses of PGMs because of coprecipitation and/or adsorption.

CONCLUSIONS

An innovative solvometallurgical process was developed and successfully applied toward near-zero waste recycling of PGMs from spent automotive catalysts. The oxidative dissolution of PGMs using organic lixiviants (*i.e.*, $FeCl_3/CH_3CN$, $CuCl_2/CH_3CN$, $FeCl_3$/DMSO, and $CuCl_2$/DMSO) depended on the temperature, leaching time, oxidizing agent concentration, and S/L ratio. Selective leaching of Pd was achieved using 0.01 mol L^{-1} $FeCl_3/CH_3CN$ followed by the total leaching of Pt and Rh with 0.3 mol L^{-1} $FeCl_3/CH_3CN$. The use of $FeCl_3/CH_3CN$ allows the selective dissolution of PGMs without harsh leaching conditions (*i.e.*, aggressive acid media and *aqua regia*) and avoids the emissions of toxic gases (Cl_2, H_2, and NO_x). The solvent CH_3CN was recovered by distillation. Furthermore, the solvoleaching of PGMs was investigated in depth by UV−vis spectra and electrochemical properties (*i.e.*, CVs and formal reduction potentials of the Fe^{3+}/Fe^{2+} and

https://dx.doi.org/10.1021/acssuschemeng.0c07355
ACS Sustainable Chem. Eng. 2021, 9, 337−350

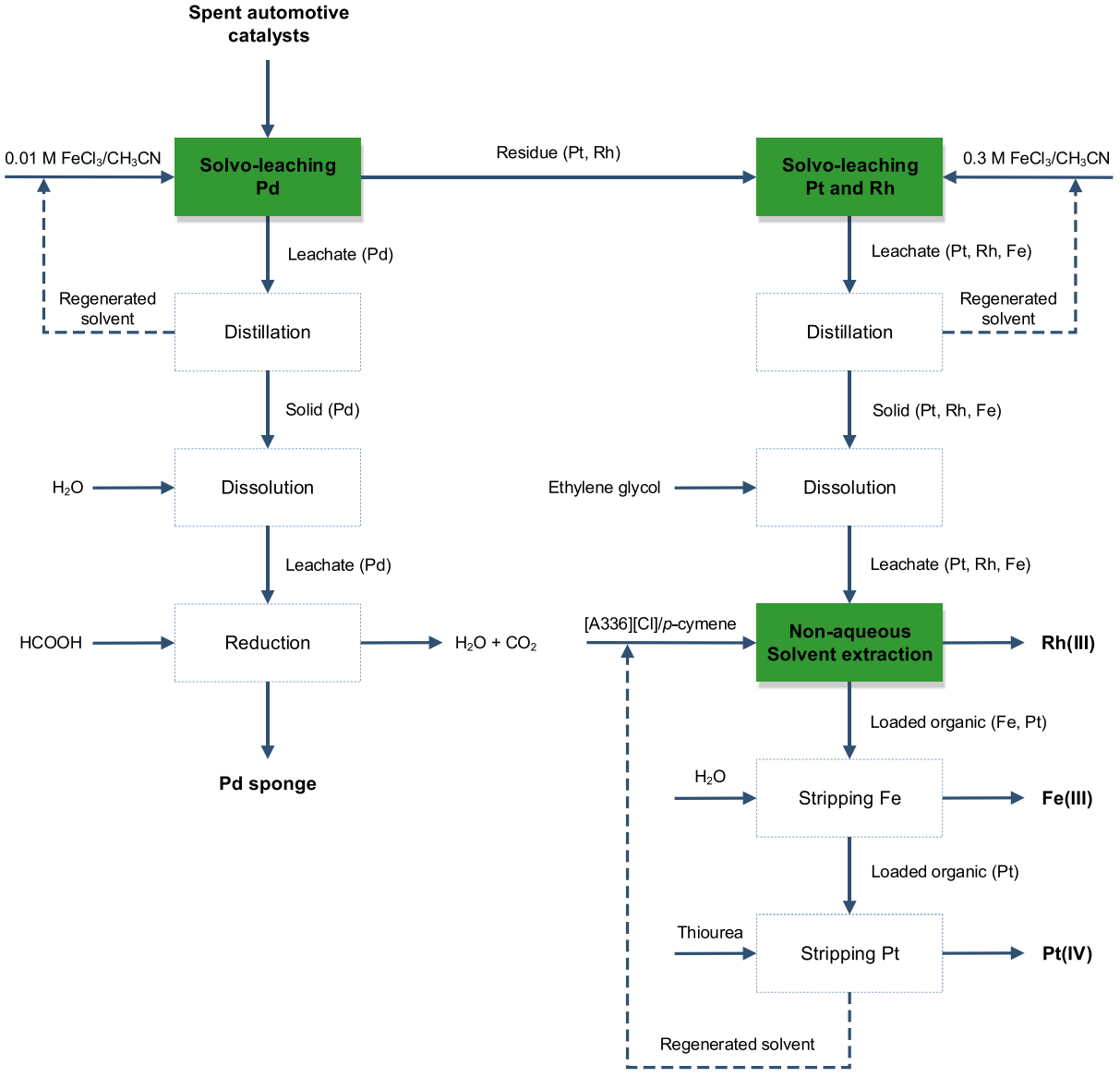

Figure 10. Conceptual flow sheet for integrated solvometallurgical leaching and nonaqueous solvent extraction for separation of PGMs from spent automotive catalysts.

Cu^{2+}/Cu^{+} couples in DMSO and CH_3CN). Subsequently, NASX using the ionic liquid [A336][Cl] diluted in the green solvent *p*-cymene was used for the separation of Fe(III) and Pt(IV) from Rh(III) in EG. The ionic liquid phase was regenerated after being selectively stripped with water and thiourea solution to recover Fe(III) and Pt(IV), respectively. The closed-loop solvometallurgical processes enable sustainable recovery of PGMs from secondary materials.

■ ASSOCIATED CONTENT

Supporting Information

The Supporting Information is available free of charge at https://pubs.acs.org/doi/10.1021/acssuschemeng.0c07355.

X-ray powder diffractometer, emission electron probe microanalyzer, electrochemical studies (CVs and formal reduction potentials of the Fe^{3+}/Fe^{2+} and Cu^{2+}/Cu^{+} couples in DMSO and CH_3CN), stripping of PGMs from loaded ionic liquids, and microwave digestion program (PDF)

■ AUTHOR INFORMATION

Corresponding Author

Koen Binnemans − *Department of Chemistry, KU Leuven, B-3001 Leuven, Belgium;* orcid.org/0000-0003-4768-3606; Phone: +3216327446; Email: Koen.Binnemans@kuleuven.be

Authors

Viet Tu Nguyen − *Department of Chemistry, KU Leuven, B-3001 Leuven, Belgium;* orcid.org/0000-0002-9348-8011

Sofía Riaño − *Department of Chemistry, KU Leuven, B-3001 Leuven, Belgium;* orcid.org/0000-0002-1049-6156

Emir Aktan − *Department of Chemistry, KU Leuven, B-3001 Leuven, Belgium*

Clio Deferm − *Department of Chemistry, KU Leuven, B-3001 Leuven, Belgium*

Jan Fransaer − *Department of Materials Engineering, KU Leuven, B-3001 Heverlee, Belgium*

Complete contact information is available at: https://pubs.acs.org/10.1021/acssuschemeng.0c07355

https://dx.doi.org/10.1021/acssuschemeng.0c07355
ACS Sustainable Chem. Eng. 2021, 9, 337−350

Notes

The authors declare no competing financial interest.

■ ACKNOWLEDGMENTS

The research leading to these results received funding from the European Union's Horizon 2020 Research and Innovation program under Grant Agreement no. 730224 (PLATIRUS). This publication reflects only the authors' view, exempting the community from any liability. The authors also thank Mehmet Ali Recai Önal for helping with the characterization of the spent automotive catalysts using XRD and EPMA.

■ REFERENCES

(1) Farrauto, R. J.; Deeba, M.; Alerasool, S. Gasoline Automobile Catalysis and Its Historical Journey to Cleaner Air. *Nat. Catal.* **2019**, *2*, 603−613.
(2) European Commission. Critical Raw Materials, 2020. https://Ec.Europa.Eu/Growth/Sectors/Raw-Materials/Specific-Interest/Critical_en (accessed April 2nd 2020).
(3) Dong, H.; Zhao, J.; Chen, J.; Wu, Y.; Li, B. Recovery of Platinum Group Metals from Spent Catalysts : A Review. *Int. J. Miner. Process.* **2015**, *145*, 108−113.
(4) Ding, Y.; Zhang, S.; Liu, B.; Zheng, H.; Chang, C.-C.; Ekberg, C. Recovery of Precious Metals from Electronic Waste and Spent Catalysts: A Review. *Resour., Conserv. Recycl.* **2019**, *141*, 284−298.
(5) Jha, M. K.; Lee, J.-C.; Kim, M.-S.; Jeong, J.; Kim, B.-S.; Kumar, V. Hydrometallurgical Recovery/Recycling of Platinum by the Leaching of Spent Catalysts: A Review. *Hydrometallurgy* **2013**, *133*, 23−32.
(6) Lee, J.-C.; Kurniawan; Hong, H.-J.; Chung, K. W.; Kim, S. Separation of Platinum, Palladium and Rhodium from Aqueous Solutions Using Ion Exchange Resin: A Review. *Sep. Purif. Technol.* **2020**, *246*, 116896.
(7) Hagelüken, C. Recycling of Electronic Scrap at Umicore's Integrated Metals Smelter and Refinery. *World Metall.—Erzmet.* **2006**, *59*, 152−161.
(8) Saguru, C.; Ndlovu, S.; Moropeng, D. A Review of Recent Studies into Hydrometallurgical Methods for Recovering PGMs from Used Catalytic Converters. *Hydrometallurgy* **2018**, *182*, 44−56.
(9) Trinh, H. B.; Lee, J.-C.; Srivastava, R. R.; Kim, S.; Ilyas, S. Eco-Threat Minimization in HCl Leaching of PGMs from Spent Automobile Catalysts by Formic Acid Prereduction. *ACS Sustainable Chem. Eng.* **2017**, *5*, 7302−7309.
(10) Baghalha, M.; Khosravian Gh, H.; Mortaheb, H. R. Kinetics of Platinum Extraction from Spent Reforming Catalysts in Aqua-Regia Solutions. *Hydrometallurgy* **2009**, *95*, 247−253.
(11) Angelidis, T. N.; Skouraki, E. Preliminary Studies of Platinum Dissolution from a Spent Industrial Catalyst. *Appl. Catal., A* **1996**, *142*, 387−395.
(12) Nagai, H.; Shibata, E.; Nakamura, T. Development of Methods for Concentration and Dissolution of Rh and Ru from Copper Slime. *Hydrometallurgy* **2017**, *169*, 282−289.
(13) Kumar, M.; Lee, J.-c.; Kim, M.; Jeong, J.; Kim, B.; Kumar, V. Hydrometallurgical Recovery/Recycling of Platinum by the Leaching of Spent Catalysts: A Review. *Hydrometallurgy* **2013**, *133*, 23−32.
(14) Nogueira, C. A.; Paiva, A. P.; Oliveira, P. C.; Costa, M. C.; da Costa, A. M. R. Oxidative Leaching Process with Cupric Ion in Hydrochloric Acid Media for Recovery of Pd and Rh from Spent Catalytic Converters. *J. Hazard. Mater.* **2014**, *278*, 82−90.
(15) Binnemans, K.; Jones, P. T. Solvometallurgy : An Emerging Branch of Extractive Metallurgy. *J. Sustain. Metall.* **2017**, *3*, 570−600.
(16) Brunzie, G. F.; Johnson, T. R.; Steunenberg, R. K. Selective Dissolution of Uranium from Uranium- Uranium Oxide Mixtures by Bromine-Ethyl Acetate. *Anal. Chem.* **1961**, *33*, 1005−1006.
(17) Trifonova, E. N.; Drobot, D. V.; Krenev, V. A. Chlorination of Metallic Rhenium by Chlorine Gas in Dimethylformamide. *Inorg. Mater.* **2003**, *39*, 529−531.
(18) Chekmarev, A. M.; Buchikhin, E. P.; Sidorov, D. S.; Koshcheev, A. M. Zirconium Dissolution by Low-Temperature Chlorination in Dimethylformamide. *Theor. Found. Chem. Eng.* **2007**, *41*, 752−754.
(19) Li, X.; Monnens, W.; Li, Z.; Fransaer, J.; Binnemans, K. Solvometallurgical Process for Extraction of Copper from Chalcopyrite and Other Sulfidic Ore Minerals. *Green Chem.* **2020**, *22*, 417−426.
(20) Li, X.; Van Den Bossche, A.; Vander Hoogerstraete, T.; Binnemans, K. Ionic Liquids with Trichloride Anions for Oxidative Dissolution of Metals and Alloys. *Chem. Commun.* **2018**, *54*, 475−478.
(21) Van Den Bossche, A.; De Witte, E.; Dehaen, W.; Binnemans, K. Trihalide Ionic Liquids as Non-Volatile Oxidizing Solvents for Metals. *Green Chem.* **2018**, *20*, 3327−3338.
(22) Nakao, Y. Dissolution of Noble Metals in Halogen-Halide-Polar Organic Solvent Systems. *J. Chem. Soc. Chem. Commun.* **1992**, *5*, 426−427.
(23) Serpe, A.; Bigoli, F.; Cabras, M. C.; Fornasiero, P.; Graziani, M.; Mercuri, M. L.; Montini, T.; Pilia, L.; Trogu, E. F.; Deplano, P. Pd-Dissolution through a Mild and Effective One-Step Reaction and Its Application for Pd-Recovery from Spent Catalytic Converters. *Chem. Commun.* **2005**, *8*, 1040−1042.
(24) Lin, W.; Zhang, R.-W.; Jang, S.-S.; Wong, C.-P.; Hong, J.-I. Il. "Organic Aqua Regia"-Powerful Liquids for Dissolving Noble Metals. *Angew. Chem., Int. Ed.* **2010**, *49*, 7929−7932.
(25) Demopoulos, G. P.; Pouskouleli, G.; Prud'Homme, P. J. A. Direct Recovery of Precious Meteals by Solvent Extraction and Selective Removal. U.S. Patent 4,654,145 A, March 31, 1987.
(26) Li, Z.; Li, X.; Raiguel, S.; Binnemans, K. Separation of Transition Metals from Rare Earths by Non-Aqueous Solvent Extraction from Ethylene Glycol Solutions Using Aliquat 336. *Sep. Purif. Technol.* **2018**, *201*, 318−326.
(27) Batchu, N. K.; Vander Hoogerstraete, T.; Banerjee, D.; Binnemans, K. Separation of Rare-Earth Ions from Ethylene Glycol (+LiCl) Solutions by Non-Aqueous Solvent Extraction with Cyanex 923. *RSC Adv.* **2017**, *7*, 45351−45362.
(28) Batchu, N. K.; Dewulf, B.; Riaño, S.; Binnemans, K. Development of a Solvometallurgical Process for the Separation of Yttrium and Europium by Cyanex 923 from Ethylene Glycol Solutions. *Sep. Purif. Technol.* **2020**, *235*, 116193.
(29) Li, Z.; Zhang, Z.; Smolders, S.; Li, X.; Raiguel, S.; Nies, E.; De Vos, D. E.; Binnemans, K. Enhancing Metal Separations by Liquid−Liquid Extraction Using Polar Solvents. *Chem.—Eur. J.* **2019**, *25*, 9197−9201.
(30) Yakoumis, I.; Moschovi, A. M.; Giannopoulou, I.; Panias, D. Real Life Experimental Determination of Platinum Group Metals Content in Automotive Catalytic Converters. *IOP Conf. Ser.: Mater. Sci. Eng.* **2018**, *329*, 012009.
(31) Jayasekera, S.; Avraamides, J.; Parker, A. Solvation of Ions. Some Applications. V Electrolytic Recovery of Silver from Non-Aqueous Solutions. *Aust. J. Chem.* **1983**, *36*, 1695−1704.
(32) Kratochvil, B.; Long, R. Iron (III)-(II) Couple in Acetonitrile Oxidation of Thiocyanate by Iron(III). *Anal. Chem.* **1970**, *42*, 43−46.
(33) Chaudhry, M.; Persson, I. Transfer Thermodynamic Study on the Copper(II) Ion from Water to Methanol, Acetonitrile, Dimethyl Sulfoxide and Pyridine. *J. Chem. Soc., Faraday Trans.* **1994**, *90*, 2243−2248.
(34) Benari, M. D.; Hefter, G. T. Electrochemical Characteristics of the Iron(III)/Iron(II) System in Dimethylsulphoxide Solutions. *Electrochim. Acta* **1991**, *36*, 471−477.
(35) Foil, A.; Le Demezet, M.; Courtot-Coupez, J. Systemes Oxydo-Reducteurs Du Cuivre Dans Le Dimethyl-Sulfoxyde. *Electroanal. Chem. Interfacial Electrochem.* **1972**, *35*, 41−54.
(36) Selbin, J.; Bull, W. E.; Holmes, L. H. Metallic Complexes of Dimethylsulphoxide. *J. Inorg. Nucl. Chem.* **1961**, *16*, 219−224.
(37) Wayland, B. B.; Schramm, R. F. Cationic and Neutral Chloride Complexes of Palladium (II) with the Nonaqueous Solvent Donors Acetonitrile, Dimethyl Sulfoxide, and a Series of Amides. Mixed Sulfur and Oxygen Coordination Sites in a Dimethyl Sulfoxide Complex. *Inorg. Chem.* **1969**, *8*, 971−976.

https://dx.doi.org/10.1021/acssuschemeng.0c07355
ACS Sustainable Chem. Eng. 2021, 9, 337−350

(38) Farha, F., Jr.; Iwamoto, R. T. Electrochemical Behavior of Copper Ions and Silver Ion in Hydracrylonitrile and Some Related Nitriles. *J. Electroanal. Chem.* **1964**, *8*, 55−64.
(39) Parker, A. J. Solvation of Ions. Applications to Minerals and Energy. *Pure Appl. Chem.* **1981**, *53*, 1437−1445.
(40) Benari, M. D.; Hefter, G. T. Electrochemical Characteristics of the Iron(III)/Iron(II) System in Dimethylsulphoxide Solutions. *Electrochim. Acta* **1991**, *36*, 471−477.
(41) Noor, N. M.; Othman, R.; Hatta, M. A. M.; Ani, M. H. Determination of Linear Tafel Region from Piecewise Linear Regression Analysis. *Int. J. Electroact. Mater.* **2014**, *2*, 22−27.

https://dx.doi.org/10.1021/acssuschemeng.0c07355
ACS Sustainable Chem. Eng. 2021, 9, 337−350